All-Chalcogenide Raman-Parametric Laser, Wavelength Converter, and Amplifier in a Single Microwire

Raja Ahmad and Martin Rochette, *Senior Member, IEEE*

Abstract—Compact, power efficient, and fiber-compatible lasers, wavelength converters, and amplifiers are vital devices for the future of fiber-optic systems and networks. Nonlinear optical effects, like Raman scattering and parametric four-wave mixing, offer a way to realize such devices. Here, we use a single chalcogenide microwire to realize a device that provides the functions of a Stokes Raman-parametric laser, a four-wave mixing anti-Stokes wavelength converter, an ultra-broadband Stokes/anti-Stokes Raman amplifier and a supercontinuum generator. The device operation relies on ultrahigh Raman and Kerr gain that are up to five orders of magnitude larger than in silica fibers, precisely engineered chromatic dispersion, and high photosensitivity of the chalcogenide microwire. Owing to the underlying principle of nonlinear optical processes, the device is anticipated to operate over the entire transmission window of the chalcogenide glass ($\lambda \sim 1$–$10\ \mu$m).

Index Terms—Fiber lasers, fiber nonlinear optics, four-wave mixing, nonlinear optical devices, optical amplifiers, optical device fabrication, optical fiber devices, optical mixing, Raman scattering, spontaneous emission, supercontinuum generation.

I. INTRODUCTION

THE future of fiber-optic systems lies in the development of all-fiber photonic devices that are compact, power efficient, and can provide novel functionalities. Optical microwires (μ-wires) are fiber waveguides with cross-section diameters in the order of the operating wavelength. The μ-wires are attractive owing to their negligible coupling and propagation losses [1], orders of magnitude enhancement in waveguide nonlinear coefficient [2], [3], controllable amount of chromatic dispersion [4] and evanescent optical field propagation [5], [6]. These advantages have driven researchers to use μ-wires for studying novel low field optical phenomena [7]–[12], as well as for wide-ranged application in the fields of nonlinear optics [4], [13], sensing [5], [6], [14] and plasmonics [9], [15]–[17], to name a few.

Optical sources, both coherent and incoherent, are among the basic components of any fiber-optic system. The former are narrowband and are usually lasers or their wavelength converted counterparts (via nonlinear wave-mixing process), while the latter are broadband, rely on spontaneous emission processes and act as the amplifiers or as broadband light sources. Recently, lasing has been reported in μ-wires made from rare-earth or dye doped silica glass [18]–[21], but these devices required pumping via evanescent coupling to the μ-wire coiled in a resonator geometry. The evanescent coupling is unfortunately an obstacle to the practical use of such lasers in fiber systems, where the large coupling and/or transmission losses of such devices is a major obstacle toward low power consumption and high power efficiency. Moreover, the gain spectrum following from discrete atomic transitions in doped silica limits the wavelength tunability of these devices.

In contrast with this, the nonlinear optical effects manifest at arbitrary wavelengths. This offers a way to circumvent the issue of wavelength tunability. The As_2Se_3 chalcogenide glass fiber exhibits nonlinear Kerr and Raman gain coefficients that are up to three orders of magnitude larger than that of silica fibers [22]. The nonlinear gain, defined as the ratio of output power to the input power, is further enhanced in a μ-wire geometry, where the optical field intensity is enhanced by more than two orders of magnitude due to the correspondingly reduced waveguide modal area. Therefore, As_2Se_3 μ-wires are excellent candidates for the development of compact and efficient sources based on nonlinear optical effects. The As_2Se_3 glass also brings the advantage of a large photosensitivity [23], enabling the direct inscription of Bragg grating (BG) reflectors within the μ-wire structure to form the laser cavity [24]. Of great importance also brought by As_2Se_3 is an ultra-wide transmission window that allows the useful operation spectrum over the wavelength range of $\lambda \sim 1$–$10\ \mu$m [25].

Recently, we made the first and only reports of lasers based on the nonlinear gain in μ-wires [26], [27], showing the use of μ-wires within a resonant cavity to generate a laser effect. It appears that the round-trip cavity losses in using the μ-wires inserted into resonant cavities could be reduced by using a completely integrated solution instead than free-space components or silica glass fiber components. Furthermore, an all-chalcogenide integrated solution would broaden the spectrum of operation of the device, up to the mid-infrared, instead than being limited to the operation spectrum of silica glass.

In this paper, we report a distributed Bragg reflector (DBR) As_2Se_3 μ-wire Raman-parametric laser, wavelength converter, amplifier, and supercontinuum generator in a single chalcogenide microwire. The resonant cavity of the device is made

The authors are with the Department of Electrical and Computer Engineering, McGill University, Montréal, QC H3A 2A7, Canada (e-mail: raja.ahmad@mcgill.ca; martin.rochette@mcgill.ca).
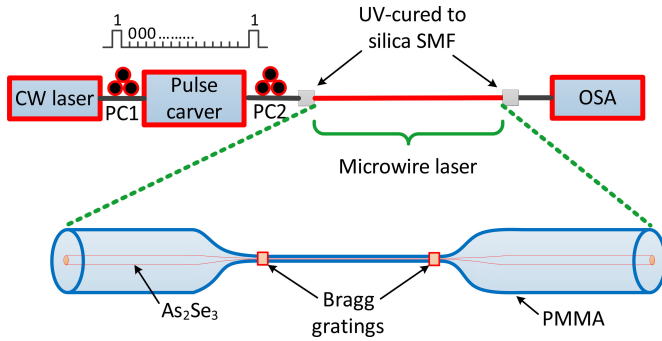
Fig. 1.   Experimental setup and device schematic. The top part shows the experimental setup for the operation of chalcogenide microwire Raman-parametric laser, wavelength converter and travelling wave amplifier. A schematic of the micro laser device is also drawn at the bottom. CW laser: continuous-wave (CW) tunable laser; PC: fiber polarization controller; SMF: single-mode fiber; OSA: optical spectrum analyzer.

out of two BGs directly written within the As_2Se_3 μ-wire, exploiting its high photosensitivity. This allows the integration of the nonlinear gain medium and the cavity mirrors in a single μ-wire, thus minimizing the cavity losses and power threshold of the laser, as well as to improve the slope efficiency. The combination of nonlinear gain and BGs in a single μ-wire also makes the device compatible with the transmission window of As_2Se_3 glass (1–10 μm). The role of the μ-wire as a travelling wave amplifier and supercontinuum generator is also investigated. In addition to providing the functionalities of a laser and wavelength converter, the resulting device thus acts as an ultra-broadband multi-order, Stokes/anti-Stokes Raman amplifier and/or a supercontinuum source.

II. DEVICE FABRICATION

Fig. 1 shows the schematic of the chalcogenide μ-wire device as well as the setup for the lasing, wavelength conversion, and amplification experiments. The fabrication of chalcogenide μ-wire device is carried out in four steps. In first step, an As_2Se_3-PMMA hybrid fiber preform is fabricated in a custom-built fiber drawing tower where a heat funnel is mounted at the top and the fiber preform is collected at the bottom. An As_2Se_3 chalcogenide fiber with a diameter of 170 μm is inserted into a PMMA tube with an inner diameter of 3.175 mm, and the two are introduced into the heat funnel heated to a temperature of 220 °C. The resulting hybrid As_2Se_3-PMMA structure is captured at the bottom and is pulled vertically to obtain the hybrid fiber preform. In a second step, the hybrid fiber preform is heated and stretched in the same drawing assembly with a different heating element, to obtain hybrid fibers with the As_2Se_3 core diameter of ∼16 μm. The PMMA coating diameter of the hybrid fiber is ∼18 times greater than that of the As_2Se_3 core and adds physical strength to the final μ-wire device, in addition to advantageously modifying the dispersion properties for the parametric nonlinear processes [13]. The As_2Se_3 core diameter of 16 μm provides optimal mode-matching to single-mode silica fibers, thus resulting in a predominantly fundamental mode excitation and a low coupling loss [28]. In a third step, a 5.5 cm long piece of the hybrid fiber is mechanically polished at both ends and stretched

into a 13 cm long μ-wire with a uniform core section using the flame-brush technique [28]. In the final step, single-mode silica fibers (SMF) pigtails are coupled to the resulting μ-wire [29]. The fundamental mode of the μ-wire has a profile optimised to match the fundamental mode of the SMF fiber. The μ-wire and the silica fibers are permanently bonded with UV-curing, thus resulting in a device compatible with standard fiber components and instruments. The μ-wire device exhibits a total (SMF-μ-wire -SMF) loss of 5.9 dB.

The diameters of the μ-wires are carefully selected to control the amount of chromatic dispersion [13], which allows the simultaneous operation of the device as a Raman-parametric laser and a FWM wavelength converter. For this purpose, the diameter of μ-wires used in the current experiment is typically around 1.0 μm.

Bragg gratings are photo-written in the μ-wire using a He-Ne laser ($\lambda = 633$ nm) interferometer assisted by a glass prism [24]. The glass prism enables setting the angle in an increased refractive index environment (BK 7 glass) to allow writing the Bragg gratings in As_2Se_3 glass (refractive index ∼2.8), which otherwise cannot be realized in free-space settings with the $\lambda = 633$ nm light. The physical length of the Bragg gratings is ∼2 mm and is adjustable by controlling the size of the interfering beams with the help of a spherical lens.

III. EXPERIMENTAL SETUP

The experimental setup consists of a laser assembly for nonlinear pumping, the μ-wire device and the OSA for output spectrum characterization. The output of a CW-laser, tunable over the C-band, is passed through a pulse-carving stage with an extinction ratio of ≥ 36 dB. The pulse carving stage consists of two cascaded 10 Gb/s Mach-Zehnder modulators (JDSU OC-192), fed with identical electrical data inputs from a pulse pattern generator (PPG). The power level of the prepared pulses is adjusted to the required levels by using a series of two EDFAs, from PriTel and two bandpass filters with <0.4 nm pass-band, followed by an optical attenuator. Depending on the operation of the μ-wire device as laser or amplifier, the duration and the repetition rate of the pump pulses is adjusted by modifying the bit pattern from the PPG. Finally, the output spectrum from the μ-wire device is observed and recorded on an OSA (Agilent 86142B).

IV. EXPERIMENTAL RESULTS

A. Broadband Amplification or Spontaneous Emission

In a first series of experiments, the μ-wires are being used as travelling wave amplifiers or a broadband source without BGs, and the impact of the μ-wire diameter is studied. Each μ-wire is 13 cm in length, and is pumped by pulses that are 100 ps in duration, have a repetition rate of 1.22 MHz and are spectrally centered at a wavelength of $\lambda = 1530$ nm. Fig. 2 shows the performance of the device as a travelling wave amplifier and as a broadband source. Fig. 2(a) shows the resulting single-pass output spectra through a 1.0 μm diameter μ-wire as a function of increasing pump power levels. The zero-dispersion
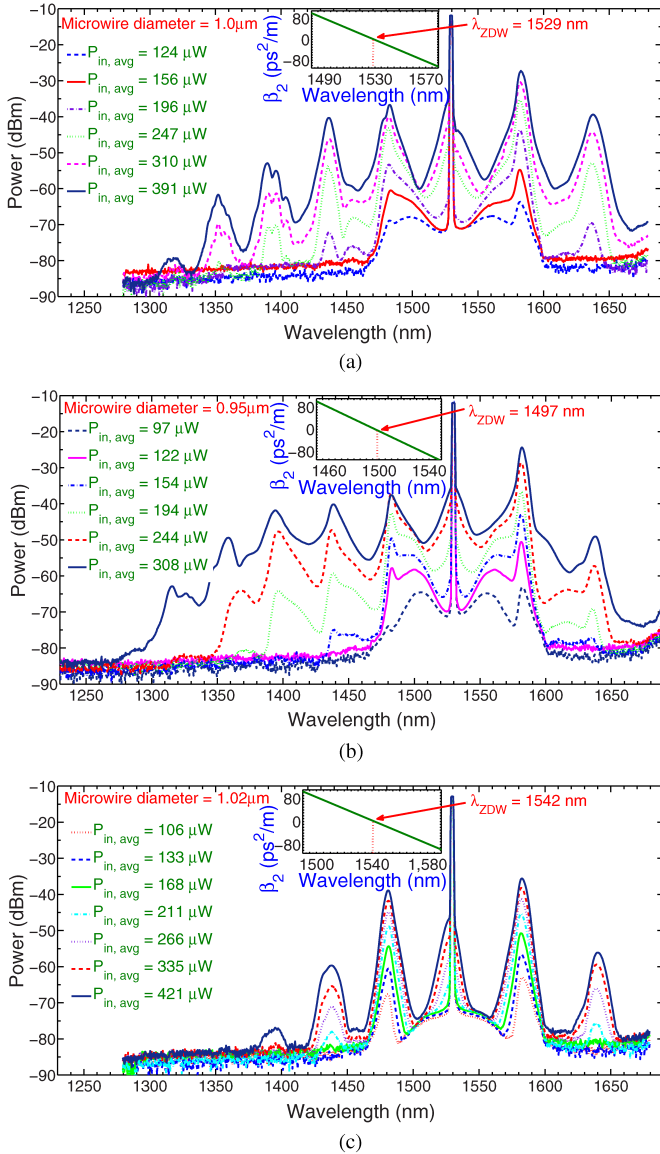
Fig. 2. Single-pass output spectra as a function of pump power in μ-wires with diameters of (a) 1.0 μm (b) 0.95 μm and (c) 1.02 μm. Numerically calculated second-order dispersion profiles of the corresponding μ-wires are included as inset in each illustration.

wavelength λ_{ZDW} of the 1.0 μm diameter μ-wire lies at $\lambda = 1529$ nm, as shown in the numerically calculated dispersion profile included in inset. This translates to the pump laser lying very close to the zero-dispersion wavelength and experiencing anomalous dispersion ($\beta_2 < 0$), thus setting up the optimal conditions for parametric interactions [30]. As a result, up to five parametrically converted output orders are observed at the anti-Stokes wavelengths, while two such converted orders are observed at the Stokes wavelengths. Additional Stokes orders are expected to lie beyond the operating wavelength range of the OSA.

The output of μ-wires is also measured when pumped away from λ_{ZDW}, both in anomalous and normal dispersion regions. The output spectrum of a μ-wire with a diameter of 0.95 μm shown in Fig. 2(b). In this case, the λ_{ZDW} is blue-shifted and

the pump lies in the anomalous dispersion wavelength region. Almost the same number of Raman orders are generated as with the 1.0 μm μ-wire. However, it is noted that the spectral energy has shifted towards shorter wavelengths, and the spectrum modulation is not as pronounced with respect to the case of the 1.0 μm diameter μ-wire. The flattening of the spectrum emerges from the anomalous dispersion pumping which favors a combination of many nonlinear optical processes (in the form of phase modulation, and wave mixing among several frequency components) and thus leads to the supercontinuum generation. The output spectrum for both 1.0 μm and 0.95 μm diameter μ-wires, spans over almost the same wavelength (frequency) range of >330 nm (>47 THz). The apparently comparable bandwidth is explained from the blue-shift of energy in the case of 0.95 μm μ-wire. To repeat the experiment on a μ-wire with normal dispersion, a μ-wire with a diameter of 1.02 μm is prepared. The spectra for this μ-wire as a function of the pump power level are provided in Fig. 2(c). As should be expected, fewer, that is up to 3 anti-Stokes orders are generated in this case, due to the input pump wavelength lying in the normal dispersion ($\beta_2 > 0$) region.

B. Raman-Parametric Lasing and Wavelength Conversion

For the laser operation, two BGs spatially apart by 11 cm are inscribed into a μ-wire with a diameter of 1.0 μm and a length of 13 cm. The reflection maxima of the two BGs are centered at $\lambda \sim 1585$ nm (L-band) with reflection coefficients of $\sim 90\%$ and 60% at the input and output ends of the μ-wire, respectively. The pump laser is centered at $\lambda \sim 1532$ nm, and the pulse duration and repetition rate are adjusted to 64 ns and ~ 3.8 kHz, respectively. The spatial extent of the pulses propagating in the μ-wire is >7.5 m, which allows the storage and/or amplification of the generated Raman/FWM gain in the μ-wire resonator for several round-trips (>34, in total) and leads to a quasi-continuous wave operation of the laser. As the device is pumped, Raman lasing is observed at a wavelength of $\lambda \sim 1585$ nm that is on the Stokes wavelength side of pump wavelength as shown in Fig. 3(a). The precise wavelength of operation of the Raman laser is defined by the central wavelength of the BGs. The FWM led-wavelength conversion is also visible at the anti-Stokes wavelength $\lambda \sim 1482$ nm. This spectrum represents the simultaneous conversion of a C-band pump laser to L- and S-bands frequency spectra. Fig. 3(b) plots the evolution of Stokes Raman and anti-Stokes FWM generated signals with increasing input pump power, revealing the respective slope efficiencies of 2.15% and 0.46%, and a threshold average (peak) pump power of ~ 52 μW (<207 mW). This represents the lowest threshold Raman laser reported to date in a fiber geometry [27], [31], and is also the first demonstration of a fully fiberized microwire laser of any kind. It is emphasized that the laser slope efficiency of $>2\%$ is a remarkably high value for such a compact, centimeters long μ-wire laser, operating at such low power levels.

Finally, we test the wavelength tunability of the lasing device. Fig. 4(a) summarizes the results of the wavelength tuning experiment. By tuning the pump wavelength over a range of

(a)

(b)
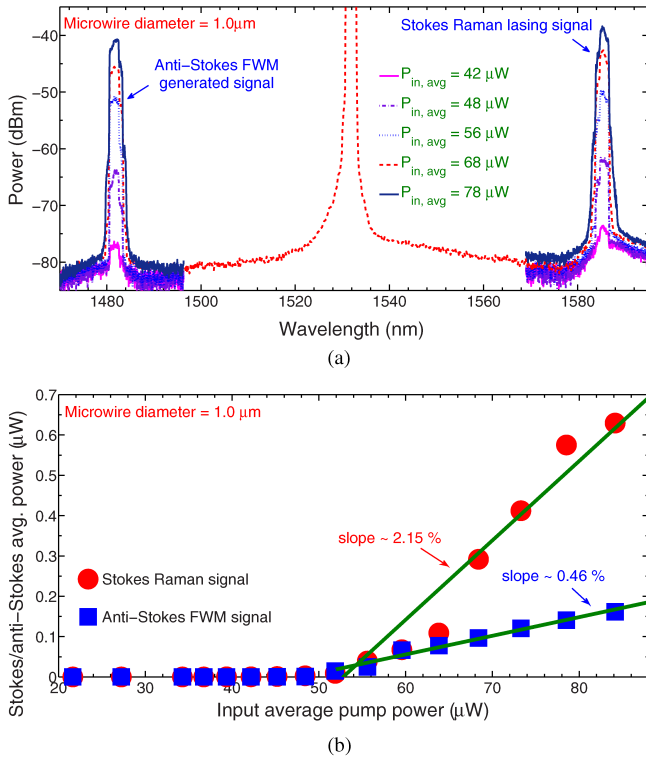
Fig. 3. Performance as a Raman-parametric laser and wavelength converter. (a) Output spectra showing the simultaneous operation of microwire Raman laser and FWM wavelength converter at different input pump power levels (b) Stokes and anti-Stokes slope efficiency curves.

(a)

(b)
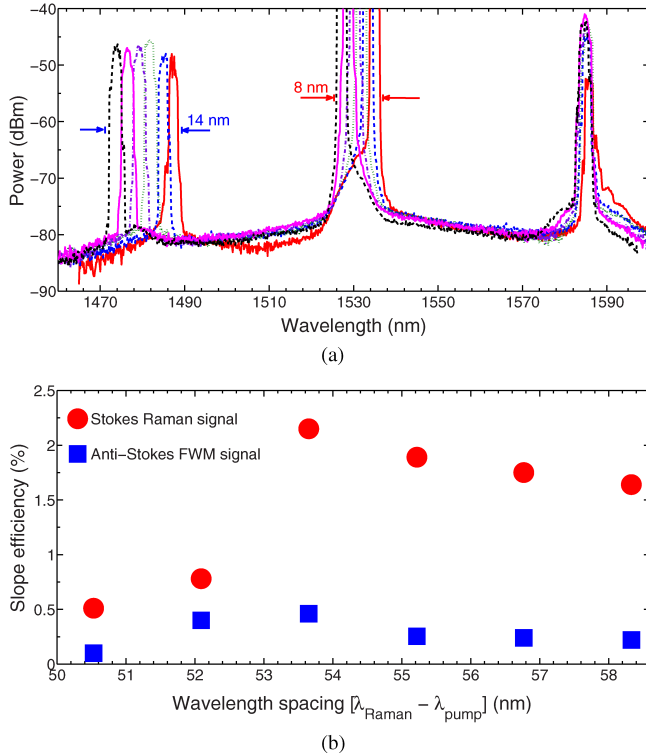
Fig. 4. Wavelength tunability of the operating device. (a) Spectra of a microwire Raman laser-FWM wavelength converter at different pump wavelengths (b) Slope efficiencies of (Stokes) Raman signal and (anti-Stokes) FWM signals for varying wavelength separation between the input pump and the resulting Raman laser.

8 nm (λ = 1527–1535 nm), the anti-Stokes output is tuned by 14 nm (λ = 1473–1487 nm), while the Stokes Raman wavelength remains fixed, bounded by the fixed resonant wavelengths of the BGs. The laser ceases to operate when the pump laser is tuned beyond the stated wavelength range of ∼8 nm, which is comparable to the Raman gain bandwidth [22]. The laser can be expected to operate so long as the Raman gain overlaps the reflection spectrum of the BGs. The asymmetric wavelength tuning between the pump laser and the anti-Stokes idler output leads from the phase matching conditions, naturally satisfied during the FWM process. The slope efficiencies of the Stokes and anti-Stokes outputs are plotted in Fig. 4(b), as a function of the wavelength separation between the pump laser and the Stokes Raman laser. The slope efficiencies are maximized for a wavelength separation of ∼53.5 nm, and decrease in value as the pump laser is detuned to either Stokes or anti-Stokes wavelengths.

V. DISCUSSION

The interplay between Raman and parametric processes in nonlinear media has been studied in the past in the context of amplification and wavelength conversion, and is reported to significantly improve the net available gain value and bandwidth in a nonlinear amplifier and wavelength converter [32]–[35]. However, the Raman-parametric lasing has never been reported yet. The device presented in this paper utilizes both Raman and parametric gains to operate simultaneously as a laser and an anti-Stokes wavelength converter. It is emphasized that the presented device is different from the reported Raman-assisted parametric amplifiers, where the Raman scattering assists in phase matching in an otherwise non-phase matched dispersive media [33]–[35]. Both Raman and parametric gains at the target wavelength are present in the μ-wire from the beginning, and merely reinforce each other into simultaneous lasing and wavelength conversion.

In order to compare the results with theory, the required threshold pump power is estimated from the roundtrip cavity loss, the effective mode area and length of the μ-wire as well as the gain coefficients of the nonlinear Raman/parametric processes. The round-trip cavity loss is 4.7 dB and includes 2.7 dB gratings reflectivity loss and a 2 dB round-trip propagation loss. The Stokes Raman signal experiences a bidirectional gain because the spatial length of the pump pulse is much longer than the laser cavity length. The round-trip gain therefore consists of two components: in forward propagation, the signal co-propagates with the pump and thus Raman-parametric gain acts on it, while in counter propagation the parametric gain is absent and the gain originates solely from the Raman effect. The total round-trip gain experienced by the signal at Stokes Raman wavelength, trapped within the laser cavity, is written as,

$$G = \exp\left(g_{\text{Raman-FWM}} L_{\text{eff}} P_{\text{pump}} + g_{\text{Raman}} L_{\text{eff}} \frac{P_{\text{pump}}}{A_{\text{eff}}} \right)$$
(1)

where P_{pump} is the input peak pump power, $L_{\text{eff}} \sim 9.7$ cm is the effective length of the μ-wire laser, corresponding to the propagation loss coefficient $\alpha \sim 10$ dB/m, and $A_{\text{eff}} = 0.51 \ \mu\text{m}^2$ is the effective transverse area of the fundamental mode in the

1.0 μm diameter μ-wire. The Raman gain coefficient for As$_2$Se$_3$ glass, as estimated in ref. [36], is $g_{\mathrm{Raman}} = 2.3 \times 10^{-11}$ m/W. The combined Raman-parametric gain coefficient $g_{\mathrm{Raman\text{-}FWM}}$ is defined as $g_{\mathrm{Raman\text{-}FWM}} = 2\gamma\Re\left[\sqrt{K(2q-K)}\right]$ [35]. Here, the term $\gamma \sim 99$ W^{-1}-m^{-1} is the effective waveguide non-linear coefficient. The term $q = 1 - f + f\chi^{(3)}(-\Omega)$, where $f = 0.1$ is the fractional contribution of Raman susceptibility to the instantaneous Kerr effect in As$_2$Se$_3$ glass [37], Ω is the angular frequency difference between the pump and the Stokes/anti-Stokes signals, and $\chi^{(3)}(\Omega)$ is the Fourier transform of the complex Raman susceptibility function, with its value for Stokes Raman shift of $\sim$6.8 THz [$\Omega = 2\pi \times 6.8 \times 10^{12}$ rad/s], calculated at $-4.28i$ for As$_2$Se$_3$ glass. Finally, the term $K = -\Delta k/2\gamma P_{\mathrm{pump}} = -\beta_2\Omega^2/2\gamma P_{\mathrm{pump}}$ is the linear phase mismatch normalized to the nonlinear contribution to the mismatch, which is from the FWM in the present case. The chromatic dispersion parameter β_2 at the pump wavelength $\lambda \sim 1532$ nm, is numerically estimated to be -5.6 ps^2/km. By using the available values, the total roundtrip gain G is evaluated from Eq. (1), as a function of peak pump power P_{pump}. The total roundtrip cavity loss of 4.7 dB estimated from the μ-wire laser parameters can be compensated with a $P_{\mathrm{pump}} \sim$ 76 mW. This value is smaller by a factor of more than 2, with respect to the measured pump peak power of the experiment. It is hypothesized that this mismatch leads from 1) the possible coupling of power to higher order modes in the μ-wire, and 2) an uncertainty in the value of pump peak power estimated from the average pump power. The uncertainty in peak power value is due to the asymmetry in temporal profile of the 64 ns duration pulse caused by the gain saturation effects in erbium-doped fiber amplifiers. Nevertheless, this indicates that in practice, the μ-wire laser presented operates with a sub-100 mW threshold pump peak power, and the experimentally estimated threshold value of 207 mW, is an over-estimate.

VI. Conclusion

In conclusion, the large Raman and parametric gain as well as the photosensitivity available in As$_2$Se$_3$ chalcogenide glass is utilized to realize a compact, low power threshold, and high efficiency, microwire Raman laser and four-wave mixing wavelength converter in simultaneous operation. A record low threshold average (peak) pump power of 52 μW (207 mW) and a slope efficiency of >2% is achieved for a $\sim$11 cm long Raman-parametric laser. The generation of combined Raman-parametric ultra-broadband spectrum is also observed, covering the wavelength (frequency) range of >330 nm (47 THz). The device is fiber-compatible and is ready for immediate use in existing fiber systems. Moreover, the laser, being all-chalcogenide and based on nonlinear optical gain, can also be readily used in the mid-infrared wavelength spectrum to cater for the current high demand of such light sources

References

[1] L. Tong, R. R. Gattass, J. B. Ashcom, S. He, J. Lou, M. Shen, I. Maxwell, and E. Mazur, "Subwavelength-diameter silica wires for low-loss optical wave guiding," *Nature*, vol. 426, no. 6969, pp. 816–818, Dec. 2003.

[2] P. Dumais, F. Gonthier, S. Lacroix, J. Bures, A. Villeneuve, P. G. J. Wigley, and G. I. Stegeman, "Enhanced self-phase modulation in tapered fibers," *Opt. Lett.*, vol. 18, no. 23, pp. 1996–1998, Dec. 1993.

[3] A. V. Shahraam and T. M. Monro, "A full vectorial model for pulse propagation in emerging waveguides with subwavelength structures—Part I: Kerr nonlinearity," *Opt. Exp.*, vol. 17, no. 4, pp. 2298–2318, Feb. 2009.

[4] T. A. Birks, W. J. Wadsworth, and P. S. J. Russell, "Supercontinuum generation in tapered fibers," *Opt. Lett.*, vol. 25, no. 19, pp. 1415–1417, Oct. 2000.

[5] G. Brambilla, "Optical fibre nanotaper sensors," *Opt. Fiber Technol.*, vol. 16, no. 6, pp. 331–342, Dec. 2010.

[6] G. Brambilla, F. Xu, P. Horak, Y. Jung, F. Koizumi, N. P. Sessions, E. Koukharenko, X. Feng, G. S. Murugan, J. S. Wilkinson, and D. J. Richardson, "Optical fiber nanowires and microwires: Fabrication and applications," *Adv. Opt. Photon.*, vol. 1, no. 1, pp. 107–161, Jan. 2009.

[7] W. She, J. Yu, and R. Feng, "Observation of a push force on the end face of a nanometer silica filament exerted by outgoing light," *Phys. Rev. Lett.*, vol. 101, no. 24, pp. 243601–1–4, Dec. 2008.

[8] G. Sagué, E. Vetsch, W. Alt, D. Meschede, and A. Rauschenbeutel, "Cold-atom physics using ultrathin optical fibers: light-induced dipole forces and surface interactions," *Phys. Rev. Lett.*, vol. 99, no. 16, p. 163602-1—163602-4, Oct. 2007.

[9] X. Guo, M. Qiu, J. M. Bao, B. J. Wiley, Q. Yang, X. Zhang, Y. G. Ma, H. K. Yu, and L. M. Tong, "Direct coupling of plasmonic and photonic nanowires for hybrid nanophotonic components and circuits," *Nano Lett.*, vol. 9, no. 12, pp. 4515–4519, Nov. 2009.

[10] E. Vetsch, D. Reitz, G. Sague, R. Schmidt, S. T. Dawkins, and A. Rauschenbeutel, "Optical interface created by laser-cooled atoms trapped in the evanescent field surrounding an optical nanofiber," *Phys. Rev. Lett.*, vol. 104, no. 20, pp. 203603–1–4, May. 2010.

[11] K. Salit, M. Salit, S. Krishnamurthy, Y. Wang, P. Kumar, and M. S. Shahriar, "Ultra-low power, zeno effect based optical modulation in a degenerate V-system with a tapered nano fiber in atomic vapor," *Opt. Exp.*, vol. 19, no. 23, pp. 22874–22881, Oct. 2011.

[12] G. Brambilla, G. S. Murugan, J. S. Wilkinson, and D. J. Richardson, "Optical manipulation of microspheres along a subwavelength optical wire," *Opt. Lett.*, vol. 32, no. 20, pp. 3041–3043, Oct. 2007.

[13] R. Ahmad and M. Rochette, "High efficiency and ultra-broadband optical parametric four-wave mixing in chalcogenide-PMMA hybrid microwires," *Opt. Exp.*, vol. 20, no. 9, pp. 9572–9580, Apr. 2012.

[14] P. Polynkin, A. Polynkin, N. Peyghambarian, and M. Mansuripur, "Evanescent field-based optical fiber sensing device for measuring the refractive index of liquids in microfluidic channels," *Opt. Lett.*, vol. 30, no. 11, pp. 1273–1275, Jun. 2005.

[15] X. W. Chen, V. Sandoghdar, and M. Agio, "Highly efficient interfacing of guided plasmons and photons in nanowires," *Nano Lett.*, vol. 9, no. 11, pp. 3756–3761, Sep. 2009.

[16] P. Wang, L. Zhang, Y. N. Xia, L. M. Tong, X. Xu, and Y. B. Ying, "Polymer nanofibers embedded with aligned Au nanorods: A new platform for plasmonic studies and optical sensing," *Nano Lett.*, vol. 12, no. 6, pp. 3145–3150, Jun. 2012.

[17] C. H. Dong, C. L. Zou, X. F. Ren, G. C. Guo, and F. W. Sun, "In-line high efficient fiber polarizer based on surface plasmon," *Appl. Phys. Lett.*, vol. 100, no. 4, pp. 041104–1–4, Jan. 2012.

[18] X. S. Jiang, Q. Yang, G. Vienne, Y. H. Li, L. M. Tong, J. J. Zhang, and L. L. Hu, "Demonstration of microfiber knot laser," *Appl. Phys. Lett.*, vol. 89, no. 14, pp. 143513–1–3, Oct. 2006.

[19] X. S. Jiang, Q. H. Song, L. Xu, J. Fu, and L. M. Tong, "Microfiber knot dye laser based on the evanescent-wave-coupled gain," *Appl. Phys. Lett.*, vol. 90, no. 23, pp. 233501–1–3, Jun. 2007.

[20] A. Sulaiman, S. W. Harun, F. Ahmad, S. F. Norizan, and H. Ahmad, "Tunable laser generation with erbium-doped microfiber knot resonator," *Laser Phys.*, vol. 22, no. 3, pp. 588–591, Mar. 2012.

[21] W. Fan, J. Gan, Z. Zhang, X. Wei, S. Xu, and Z. Yang, "Narrow linewidth single frequency microfiber laser," *Opt. Lett.*, vol. 37, no. 20, pp. 4323–4325, Oct. 2012.

[22] R. E. Slusher, G. Lenz, J. Hodelin, J. Sanghera, L. B. Shaw, and I. D. Aggarwal, "Large Raman gain and nonlinear phase shifts in high-purity As$_2$Se$_3$ chalcogenide fibers," *J. Opt. Soc. Amer. B.*, vol. 21, no. 6, pp. 1146–1155, Jun. 2004.

[23] B. J. Eggleton, B. Luther-Davies, and K. Richardson, "Chalcogenide pho-tonics," *Nat. Photon.*, vol. 5, no. 3, pp. 141–148, Feb. 2011.

[24] R. Ahmad, M. Rochette, and C. Baker, "Fabrication of Bragg gratings in subwavelength diameter As_2Se_3 chalcogenide wires," *Opt. Lett.*, vol. 36, no. 15, pp. 2886–2888, Jul. 2011.

[25] I. D. Aggarwal and J. S. Sanghera, "Development and applications of chalcogenide glass optical fibers at NRL," *J. Optoelectron. Adv. Mater.*, vol. 4, no. 3, pp. 665–678, Sep. 2002.

[26] R. Ahmad and M. Rochette, "Chalcogenide microwire based raman laser," *Appl. Phys. Lett.*, vol. 101, no. 10, pp. 101110–1–3, Sep. 2012.

[27] R. Ahmad and M. Rochette, "Raman lasing in a chalcogenide microwire-based Fabry–Perot cavity," *Opt. Lett.*, vol. 37, no. 21, pp. 4549–4551, Nov. 2012.

[28] C. Baker and M. Rochette, "High nonlinearity and single-mode trans-mission in tapered multi-mode As_2Se_3-PMMA fibers," *IEEE Photon. J.*, vol. 4, no. 3, pp. 960–969, Jul. 2012.

[29] C. Baker, R. Ahmad, and M. Rochette, "Simultaneous measurement of the core diameter and the numerical aperture in dual-mode step-index optical fibers," *J. Lightw. Technol.*, vol. 29, no. 24, pp. 3834–3837, Dec. 2011.

[30] G. P. Agrawal, *Nonlinear Fiber Optics*, 4th ed. New York, NY, USA: Academic, 2007.

[31] J. Shi, S.-U. Alam, and M. Ibsen, "Sub-watt threshold, kilohertz-linewidth raman distributed-feedback fiber laser," *Opt. Lett.*, vol. 37, no. 9, pp. 1544–1546, May 2012.

[32] N. Bloembergen and Y. R. Shen, "Coupling between vibrations and light waves in raman laser media," *Phys. Rev. Lett.*, vol. 12, no. 18, pp. 504–507, May. 1964.

[33] T. Sylvestre, H. Maillotte, E. Lantz, and P. Tchofo Dinda, "Raman-assisted parametric frequency conversion in a normally dispersive single-mode fiber," *Opt. Lett.*, vol. 24, no. 22, pp. 1561–1563, Nov. 1999.

[34] C. J. S. De Matos, D. A. Chestnut, P. C. Reeves-Hall, and J. R. Taylor, "Continuous-wave-pumped raman-assisted fiber optical parametric am-plifier and wavelength converter in conventional dispersion-shifted fiber," *Opt. Lett.*, vol. 26, no. 20, pp. 1583–1585, Oct. 2001.

[35] S. Coen, D. A. Wardle, and J. D. Harvey, "Observation of non-phase-matched parametric amplification in resonant nonlinear optics," *Phys. Rev. Lett.*, vol. 89, no. 27, pp. 273901–1–273901-4, Dec. 2002.

[36] A. Tuniz, G. Brawley, D. J. Moss, and B. J. Eggleton, "Two-photon ab-sorption effects on Raman gain in single mode As_2Se_3 chalcogenide glass fiber," *Opt. Exp.*, vol. 16, no. 22, pp. 18524–18534, Oct. 2008.

[37] J. Hu, C. R. Menyuk, L. B. Shaw, J. S. Sanghera, and I. D. Aggarwal, "Maximizing the bandwidth of supercontinuum generation in As_2Se_3 chalcogenide fibers," *Opt. Exp.*, vol. 18, no. 7, pp. 6722–6739, Mar. 2010.

Raja Ahmad is currently working toward the Ph.D. degree at McGill University, Canada. His Ph.D. research includes the nonlinear applications of chalcogenide glass microwires. He has authored/coauthored 26 papers including 16 journal papers.

Martin Rochette is an Associate Professor at the Department of Electrical and Computer Engineering, McGill University. He published more than 130 journal and conference papers on highly nonlinear materials and devices, fiber laser sources, optical fiber components, and optical communication systems. His cur-rent research interests include the application of nonlinear effects for devices and laser sources with applications for sensors, instrumentation, telecommuni-cation systems, and biomedicine.